BIOCHEMISTRY
including biophysical chemistry & molecular biology
Article

Biochemistry **2010,** *49,* 6365–6374 6365
DOI: 10.1021/bi100047n

Structural and Functional Analysis of the C-Terminus of Gαq in Complex with the Human Thromboxane A_2 Receptor Provides Evidence of Constitutive Activity[†]

Annirudha Chillar, Jiaxin Wu, Vanessa Cervantes, and Ke-He Ruan*

Center for Experimental Therapeutics and Pharmacoinformatics, Department of Pharmacological and Pharmaceutical Sciences, University of Houston, Houston, Texas 77204

Received January 12, 2010; Revised Manuscript Received June 29, 2010

ABSTRACT: The human thromboxane A_2 (TXA_2) receptor (TP) is known to mediate platelet aggregation and vasoconstriction. The receptor predominantly interacts with the Gq protein, thereby activating phospholipase C and increasing the intracellular calcium level. In this study, we synthesized a 15-residue peptide corresponding to the C-terminal domain of the Gq protein α subunit (Gαq-Ct peptide) and characterized its interaction with recombinant TP purified from a baculovirus expression system in the presence and absence of an agonist using fluorescence and NMR spectroscopic studies. With fluorescence binding assays, we demonstrated that the Gαq-Ct peptide was bound to TP, in the absence of the agonist, with a K_d value of approximately 17 μM. Interestingly, upon addition of the agonist, U46619, the Gαq-Ct peptide's binding affinity for this activated TP was reduced, thereby increasing the K_d value to approximately 240 μM. NMR experiments demonstrated that the TP-bound Gαq-Ct peptide shows a different affinity and conformation, in the absence and presence of the agonist, U46619. This suggested there is the possibility of ligand-free constitutive TP signaling through Gα binding. Thus, an HEK293 cell line that stably expresses human TP and lacks the ability to produce TXA_2 was created by gene transfer and G418 selection. In comparison with the control cells, the stable cell line showed significant Gα-mediated ligand-free calcium signaling. The study indicates a promising new outlook for the examination of prostanoid receptor−G-protein interactions in greater detail using integrated NMR spectroscopy, the purified receptor, and the stable cell line.

Prostanoids, comprising prostaglandins and thromboxane, make up a family of bioactive oxygenated metabolites of arachidonic acid. They act as local hormones in the vicinity of their production site and regulate the local homeostasis (*1*−*4*). Each prostanoid exerts its function by binding to a specific prostanoid receptor. All known prostanoid receptors belong to the G-protein-coupled receptor (GPCR) family, possessing a common membrane topology of seven transmembrane (TM) domains (*5*).

The human thromboxane A_2 (TXA_2)[1] receptor (TP) was originally purified from placenta in 1989, and its cDNA was cloned in 1991 (*6*, *7*). There are two isoforms of TP with different C-terminal tails resulting from alternative splicing. It has been widely accepted that TP predominantly couples to the Gq type of G-protein upon ligand stimulation and activates phospholipase C with a subsequent increase in inositol triphosphate, diacylglycerol, and intracellular free calcium concentrations (*8*−*10*). However, very little is known about the mechanisms for coupling between TP and the Gq proteins from a structural point of view.

To quantify the efficacy of the drugs targeting GPCRs, various GPCR theories in pharmacology have been hypothesized according to experimental data obtained from the studies of mutagenesis, fusion proteins, and stimulus-biased cell lines (*11*). In contrast to the quickly evolving pharmacological receptor theories, little structural information is available to confirm these models and provide detailed insight into how the coupling between G-protein and different receptor states actually occurs. From all the GPCRs, high-resolution crystallographic structures are available for only rhodopsin, the adenosine A_{2A} receptor, and the β-1 and β-2 adrenergic receptors. This is mostly due to the difficulties in overexpression, purification, and crystallization of membrane proteins. Characterizing the interaction between the GPCR and G-protein by a crystallographic approach requires the cocrystallization of the receptor and the G-protein, which will be even more complex than the crystallization of the receptor itself. NMR spectroscopy has been used to study the interaction between rhodopsin and a C-terminal fragment of transducin (Gt). The results suggested that rhodopsin, without light activation, could not bind to Gt, which is similar to the original ternary complex model prediction (*12*). It is clear that the details of the interaction between G-proteins and GPCRs need to be further characterized.

Several crystal structures of the Gαq protein have been determined. The first reported crystal structure does not include the C-terminal fragment (*13*). One recently determined crystal structure (*14*) does have a complete C-terminal fragment; however, its C-terminal fragment is in contact with a guanine nucleotide exchange factor protein. Thus, its 3D structure might not be the same as that of a GPCR-bound structure. Because site-directed mutagenesis and NMR studies all indicate that the C-terminal fragments of all the G-proteins are important, thus making the GPCR-binding epitopes important determinants for

[†]This work was supported by National Institutes of Health Grants HL56712 and HL79389 to K.-H.R.

*To whom correspondence should be addressed: 4800 Calhoun Rd., Room 521, SR2 Bldg., Houston, TX 77204-5037. Telephone: (713) 743-1771. Fax: (713) 743-1884. E-mail: khruan@uh.edu.

[1]Abbreviations: TXA_2, thromboxane A_2; TP, TXA_2 receptor; Gαq, heterotrimeric G-protein q α subunit; Gαq-Ct peptide, Gαq C-terminal peptide; DQF-COSY, double-quantum-filtered correlation spectroscopy; NOE, nuclear Overhauser effect; Sf9, *Spodoptera frugiperda*; 1D, one-dimensional; 2D, two-dimensional; 3D, three-dimensional; DG II, Distance Geometry II.

Published on Web 06/30/2010

the selectivity of G-proteins (*12*, *15*−*20*), monitoring the interaction between the TP and Gq protein should yield interesting results. Recently, we successfully purified a recombinant TP expressed in *Spodoptera frugiperda* (Sf9) insect cells (*21*). In this study, we used a C-terminal fragment of Gαq to interact with the purified TP and studied this interaction using fluorescence microscopy and fluorescence and NMR spectroscopic techniques.

EXPERIMENTAL PROCEDURES

Materials. D_2O was purchased from Cambridge Isotope Laboratory (Andover, MA). β-D-Dodecyl maltoside (DM) was purchased from CALBIOCHEM (San Diego, CA). U46619 (a TP agonist) was from Cayman Chemicals (Ann Arbor, MI). [^{3}H]U46619 and [^{3}H]SQ29,548 (a TP antagonist) were from NEN (PerkinElmer, Waltham, MA). Fluo8-AM dye was purchased from ABD bioquest. All other reagents were purchased from Sigma-Aldrich (St. Louis, MO) and Bio-Rad (Hercules, CA).

Peptide Synthesis. A peptide corresponding to the 15 residues of the C-terminal domain of Gαq (KDTILQLNLKEYNLV, termed the Gαq-Ct peptide) was synthesized by Sigma-Genosys. The crude peptide was purified by HPLC using a C4 reverse-phase column, and the correct molecular mass of the purified peptide was verified by mass spectrometric analysis. Various studies have validated the method of use of the Gαq-Ct peptide in systems such as the rhodopsin/transducin system (*22*−*30*).

Overexpression and Partial Purification of the TP Protein. The details of receptor overexpression with the baculovirus/Sf9 cell system and purification of the active TP protein were described previously (*21*). Briefly, the cotransfection of the cultured Sf9 insect cells was performed using the wild-type Autographa Californica nuclear polyhedrosis virus (AcNPV) and the pVL1392 plasmid carrying the TP gene. The recombinant baculovirus generated by the homologous recombination was isolated, purified, and used to infect the Sf9 cells. The cells expressing the TP protein were then grown in Grace's Insect Medium supplemented with 10% fetal bovine serum. After cell harvest, the TP protein was purified by receptor-rich membrane preparation, *n*-dodecyl β-D-maltoside (DM) extraction, and high-yield FPLC gel filtration (*21*).

Determination of the Specific Ligand Binding Activity for the Purified TP Protein. [^{3}H]SQ29,548 (antagonist) and [^{3}H]U46619 (agonist) were used to bind with the TP protein in different purification steps following the detailed procedure described previously (*21*). The TP protein concentration and purity at each purification step were evaluated by SDS−PAGE and Western blot analyses (*21*). The fractions with the highest specific activity (the highest ligand binding activity with the lowest protein concentration) were concentrated and quickly dialyzed against ultrapure water (within 2 h) to reduce the salt concentration and then used for NMR and fluorescence spectroscopic experiments.

Fluorescence Studies. The changes in the intrinsic fluorescence intensity of the active TP were measured in the absence and presence of agonist U46619 and antagonist SQ29,548 with different amounts of the Gαq-Ct peptide using a Hitachi F-4500 fluorescence spectrophotometer; 0.6 mL of the purified TP (6.7 μM) in PBS containing 0.5 mM DM was titrated with different amounts of the Gαq-Ct peptide. The excitation wavelength was set at 292 nm to measure the intrinsic signal of Trp residues (nine Trp residues in the TP sequence) in the TP protein and to minimize the interference from the Tyr residues (six Tyr residues in the TP sequence) in the Gαq-Ct peptide. An emission scan from 310 to 500 nm was monitored during the peptide titration to the TP protein at room temperature in a 1.0 cm path length cell

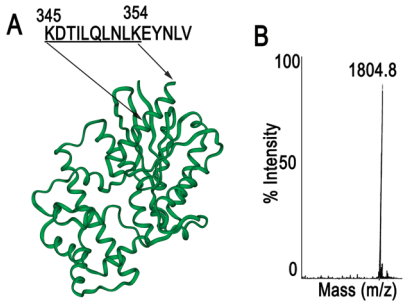

FIGURE 1: Gαq-Ct peptide mimicking the C-terminal domain of Gαq. The sequence of the peptide corresponding to the Gαq-Ct peptide that was used in this study is shown above the crystal structure of Gαq (Protein Data Bank entry 2bcj) in panel A. Its molecular mass (determined by mass spectroscopy) is shown in panel B.

(*31*). TP with buffer and scrambled peptide (KVDLTNIYLEQKLLN) was used as a control [Figure 2A(2),B(3)].

NMR Experiment. The purified Gαq-Ct peptide was dissolved in pure water (containing 5% D_2O and 0.5 mM DM) at a concentration of 2.2 mM. 1D ^{1}H and 2D DQF-COSY, TOCSY, and NOESY spectra were recorded to obtain the resonance assignments and to determine its 3D structure (*32*).

For the NMR studies of the interaction between the Gαq-Ct peptide and the TP, 0.45 mL of the purified TP (40 μM, using 5% D_2O for the lock signal) with or without U46619 was titrated with different amounts of the Gαq-Ct peptide dissolved in water. The 1D ^{1}H spectra were recorded during the titration. The final mixture of the titration, containing Gαq-Ct peptide (1.1 mM), was used for the 2D TOCSY and NOESY experiments (*33*−*36*).

All NMR experiments were conducted on a Bruker Avance 600 MHz NMR spectrometer with a 5 mm Quadra-resonance cryo-probe at 293 K. The water peak was suppressed by the Excitation Sculpting method (*37*). All 1D spectra contained 8K data points. NOESY and TOCSY spectra contained 2048 × 512 data points, and DQF-COSY spectra contained 4096 × 512 data points. For the experiments with the free Gαq-Ct peptide, NOESY was conducted with a mixing time of 300 ms. For the experiments with the peptide in the presence of unstimulated and U46619-stimulated TP, NOESY was conducted with a mixing time of 150 ms. The TOCSY spectra were recorded with the MLEV-17 spin-lock pulse sequence with a total mixing time of 70 ms. Quadrature detection was achieved in F_1 (frequency 1) by the States−TPPI method (*38*). The NMR data were processed using Felix 2000 (Accelrys, San Diego, CA). Shifted sine-bell window functions of 0° (for DQF-COSY), 70° (for TOCSY), or 90° (for NOESY) were used in both dimensions. The chemical shift was referenced to the internal standard DSS (contained in D_2O).

NMR Assignment and Determination of the Structure of the Three Gαq-Ct Conformations. The 2D homonuclear sequential assignment procedure was used to analyze the NMR data (*32*). The spin systems were identified by DQF-COSY and TOCSY; sequential assignment was then made by NOESY. After the sequential assignment, the NOE cross-peaks were assigned, and the peak volumes were measured and converted into distance constraints using Felix 2000. The distance bound method was used to generate the distance constraints. The strong, medium, and weak NOE cross-peaks were set to correspond to the upper bound distances of 2.7, 3.5, and 6.0 Å, respectively. The distance constraints were then exported into Insight II, and the 3D structures of the free Gαq-Ct peptide and TP-bound Gαq-Ct peptide were calculated using the Distance Geometry II (DG II) module.

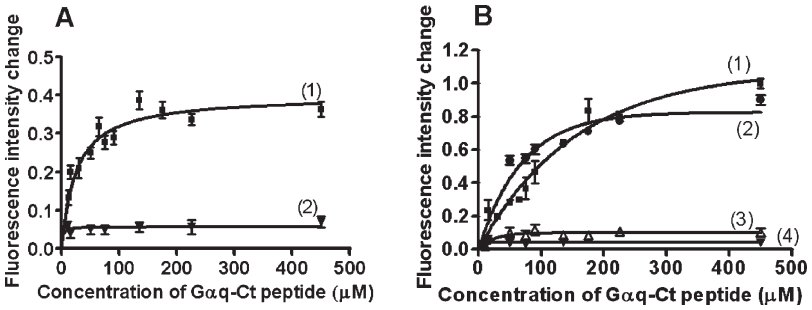

FIGURE 2: Gαq-Ct peptide binding to the purified TP as determined by fluorescence spectroscopy. The changes in the intrinsic Trp fluorescence intensity of the TP without [A(1)] or with [B(1)] U46619, upon addition of different concentrations of the Gαq-Ct peptide, normalized by the original fluorescence intensity of the TP, were plotted. A(2) shows data for the TP with the scrambled Gαq-Ct peptide (KVDLTNIYLEQKLLN) in the absence of agonist. B(2) shows data for the TP with the Gαq-Ct peptide in the presence of antagonist SQ29,548. B(3) shows data for TP with the scrambled Gαq-Ct peptide in the presence of agonist U46619. B(4) shows data for the TP with a buffer control. The K_d was estimated by fitting the data into a one-site binding model using Origin version 6.1.

The conformations of Gαq-Ct in the free state, the TP-bound state, and the ligand-activated TP-bound state were obtained.

Generation of HEK293 Cell Lines Expressing the Recombinant TP. HEK293 cells were cultured in a 100 mm cell culture dish with high-glucose Dulbecco's modified Eagle's medium (containing 10% fetal bovine serum and antibiotic and antimycotic) and were grown at 37 °C in a humidified 5% CO_2 incubator. The recombinant TP was expressed in HEK293 cells using the pcDNA3.1 vector. Briefly, the cells were grown and transfected with the purified cDNA of the recombinant TP protein by the Lipofectamine 2000 method (*39*) following the manufacturer's instructions (Invitrogen). The transfected cells were cultured in the presence of Geneticin (G418 screening) for several weeks following the manufacturer's instructions (Invitrogen). The cells stably expressing the human TP were identified by an enzyme assay and Western blot analysis.

Western Blot Analysis. Transfected HEK293 cells were washed with PBS [0.01 M phosphate buffer (pH 7.4) containing 0.15 M NaCl] and collected by centrifugation. After being washed three times, the pellet was resuspended in a small volume of the same buffer. Protein estimation was performed using fluorescence spectroscopy. Each protein sample (20 μg) was separated by 10% polyacrylamide gel electrophoresis under denaturing conditions and then transferred to a nitrocellulose membrane. Bands recognized by the particular primary polyclonal antibody for the TP were visualized with a horseradish peroxidase-conjugated secondary antibody and chromogenic peroxidase substrate.

Calcium Signaling Assay. The TP calcium signaling assay was performed on the HEK293 cells using Fluo8-AM dye. The cells were cultured in glass bottom plates and incubated with Fluo8-AM dye dissolved in Modified Hank's buffered salt solution (HBSS, without Ca^{2+} or Mg^{2+}) containing 10 mM HEPES (pH 7.6) and 0.1% bovine serum albumin (HBSSHB buffer) for 20 min. The cells were then washed with the buffer containing HBSSHB with probenecid acid (2.5 mM) and Pluronic F-68 (0.1%) and incubated for 10 min. After the cells had been washed, Gq-mediated calcium signaling was monitored with a Nikon Eclipse Ti-S fluorescence microscope using a 40× objective. The fluorescence intensity that resulted from the influx of calcium bound to the Fluo8-AM preloaded within the cells was recorded and analyzed using the software (NIS elements, Melville, NY).

RESULTS

Peptide Design, Synthesis, and Purification. The C-terminal domain of Gαq (Figure 1A) binding to human TP, which mediates the receptor signaling in cells, has been investigated by experiments that use a mini-gene technique. The mini-gene expressed 11-residue peptide, corresponding to the Gαq C-terminal domain, demonstrated the biological activity of competitive blocking in the coupling between Gαq and the TP in the cells (*40*). However, little information is available to reveal the molecular mechanism of how Gαq binds to the TP with and without ligand activation. Determination of the detailed interaction between the C-terminal domain of Gαq and purified TP in solution represents one of the key steps toward uncovering the receptor−G-protein coupling mechanisms. A peptide, corresponding to the last 15 residues of Gαq, which includes the 11-residue encoded amino acid sequence of the mini-gene, was synthesized. The peptide, which was water-soluble, was easily purified by a single-step HPLC purification using a C4 column. The correct molecular mass of the purified peptide was confirmed by mass spectrometric analysis (Figure 1B).

Expression, Solubilization, and Purification of Recombinant Human TP. An effective purification method for the preparation of the active TP protein has been developed by us previously (*21*). The full-length, glycosylated TP was expressed in Sf9 cells using a baculovirus expression system. We have developed a simple, quick, and high-yield purification approach for the TP purification (*21*). Briefly, the DM detergent was used to effectively extract the TP protein from the Sf9 cells, but the DM-extracted TP protein was contaminated with DNA as evidenced by UV and CD spectroscopic analyses. To minimize the DNA contamination, DNAase was used to break down the DNA into small pieces. The purity of the DM-extracted TP reached approximately 20% of the total protein following the purification by ultracentrifugation. We found that the optimized FPLC purification, using the Superdex-75 column with a slow flow rate, was very effective in further separating the DM-solubilized TP protein from other membrane proteins as well as the broken down DNA fragments. The purified TP from the developed procedures showed a single major band via SDS−PAGE and Western blot analyses, with a specific ligand binding ratio of 1:0.8 ([^{3}H]SQ29,548:TP molecule) (*21*).

Fluorescence Studies of the Interaction between the Gαq-Ct Peptide and TP in the Presence and Absence of the Receptor Agonist U46619 and Antagonist SQ29,548. Before the time-consuming NMR experiment, fluorescence spectroscopy was used to study the interaction between the Gαq-Ct peptide and the purified TP. The intrinsic Trp fluorescence intensity of the ligand-free TP and the U46619-activated TP changed upon the addition of the Gαq-Ct peptide. The changes in fluorescence

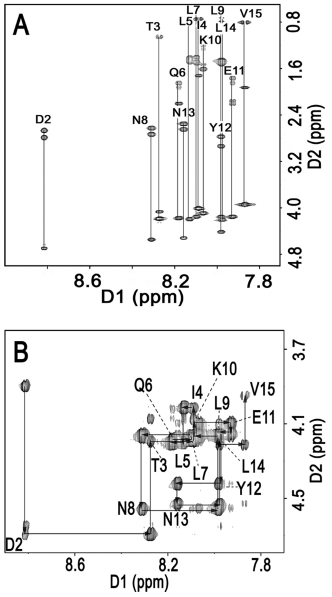

FIGURE 3: TOCSY and NOESY spectra showing spin systems and peptide assignments. (A) Expanded TOCSY spectrum showing the identification of the spin systems. (B) NOESY spectrum showing the sequential $d_{\alpha N(i,i+1)}$ peaks of the free Gαq-Ct peptide.

intensity in the presence of different concentrations of the Gαq-Ct peptide are plotted in Figure 2. The data, which were fitted into a one-site binding model, showed an apparent K_d value of 17 μM for the ligand-free TP [Figure 2A(1)] and 240 μM for the U46619-activated TP [Figure 2B(1)]. The antagonist SQ29,548 showed an apparent K_d of 92 μM with the Gαq-Ct peptide [Figure 2(B)2]. The control scrambled peptide (KVDL-TNIYLEQKLLN) did not exhibit any change in fluorescence intensity in the presence [Figure 2B(3)] or absence [Figure 2A(2)] of agonist. These results are interesting since they showed that the Gαq-Ct peptide binds to a ligand-free TP with an affinity higher than that for binding to an agonist-activated TP. The control of TP with buffer did not show any change in fluorescence intensity [Figure 2B(4)].

Determination of the Solution Structure of the Free Gαq-Ct Peptide. Because the structure of the last five residues in the Gαq C-terminal domain is not available in the Gαq crystal structure that is bound to a GPCR, we used 2D ^{1}H NMR spectroscopy to determine the solution structure of Gαq-Ct before studying its interaction with the purified TP protein. The amino acid spin systems were clearly identified from the TOCSY spectrum (Figure 3A), and the sequential assignments for the peptide were obtained from the NOESY spectrum (Figure 3B). The complete resonance assignments of HN, Hα, Hβ, and others in the free Gαq-Ct peptide are listed in Table 1. On the basis of the analysis of our NMR spectra, the free Gαq-Ct peptide forms a typical helix structure, characterized by clearly identifiable medium-range NOEs (data not shown). DG II calculation also allowed for a well-defined helix (Figure 4A). The number of constraints per residue is summarized in Figure 7A. Fifty initial structures were calculated using DG II, and the 10 structures with the smallest rmsd (root-mean-square deviation) were chosen. The rmsd for the structures of the free Gαq-Ct peptide was 1.2 Å, and the average energy for the structures was 179 kcal/mol. This solution structure of the Gαq-Ct peptide is slightly different than the crystallographic structure of Gαq at its first three residues, due to the higher flexibility of the peptide versus that of its counterpart

Table 1: Proton Chemical Shifts for the Free Gαq-Ct Peptide

residue	HN	Hα	Hβ	others
Lys1		3.897	1.800	1.584, 1.310, 2.880, 7.417
Asp2	8.815	4.636	2.680, 2.797	
Thr3	8.273	4.206	4.069	1.076
Ile4	8.087	4.030	1.741	1.350, 1.076, 0.763, 0.704
Leu5	8.131	4.206	1.487	1.447, 0.802, 0.743
Gln6	8.180	4.186	1.936, 1.858	2.210
Leu7	8.097	4.166	1.506	1.428, 0.773, 0.719
Asn8	8.307	4.558	2.738, 2.641	
Leu9	7.984	4.166	1.526	1.487, 0.802, 0.743
Lys10	8.067	4.108	1.623	1.232, 1.291, 7.388, 2.841
Glu11	7.926	4.166	1.858, 1.780	2.230, 2.171
Tyr12	7.979	4.421	2.954, 2.797	6.992, 6.684
Asn13	8.155	4.519	2.660, 2.562	
Leu14	7.975	4.225	1.526	1.487, 0.802, 0.743
Val15	7.872	3.951	1.936	0.821, 0.807

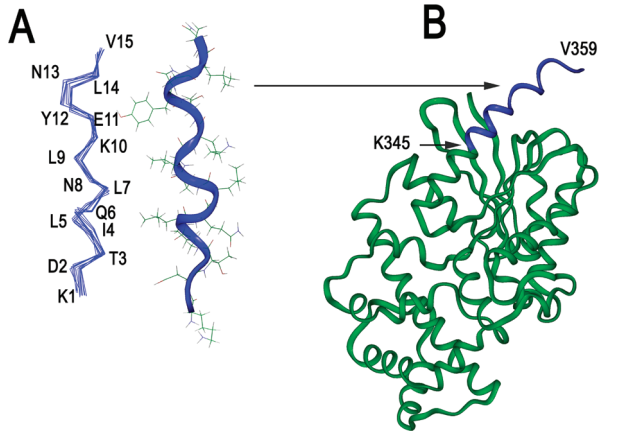

FIGURE 4: Ligand-free 3D structures of the Gαq-Ct peptide. (A) 3D structure generated from DG II and molecular dynamics calculations for the free Gαq-Ct peptide in α-carbon mode (left) or with the side chains (right). (B) This solution structure was combined with the crystal structure of Gαq to make a complete structure.

in the protein. The middle structure part of the Gαq-Ct peptide matches the crystal structure well. The last five residues at the C-terminus, which are not present in the crystal structure, show a helical structure in continuation from the middle part. These data show a complete Gαq 3D structure via configuration of the determined C-terminal structure to the X-ray structure, which lacks the defined structure for the last six residues (K354−V359, corresponding to K10−V15 in the peptide) (Figure 4B).

NMR Study of the Interaction between the Gαq-Ct Peptide with Agonist-Free TP in a Lipid Environment. To further study the interaction between the Gαq-Ct peptide and the ligand-free TP and determine its bound 3D structure, we performed the 2D proton NMR experiments for the Gαq-Ct peptide in the presence of the purified receptor. The complete resonance assignments of HN, Hα, Hβ, and others for the Gαq-Ct peptide in the presence of agonist-free TP are summarized in Table 2. Via analysis of the TOCSY spectra, it was interesting to discover that both fast and slow exchange behaviors between the free and bound peptide were observed for the NMR signals of the peptide upon its interaction with TP (Figure 5). One of the residues that exhibited a typical fast exchange as characterized by only one set of shifted peaks was residue I4 within the N-terminal segment of the Gαq-Ct peptide (Figure 5A). The significant change (0.078 ppm) in the chemical shift from 8.087 ppm [free Gαq-Ct peptide

Table 2: Proton Chemical Shifts for the Gαq-CT Peptide in the Presence of Agonist-Free TP

residue	HN	Hα	Hβ	others
Lys1		3.858	1.565,	1.776, 1.355, 2.870, 7.417
Asp2	8.785	4.675	2.734, 2.594	
Thr3	8.247	4.114	4.044	1.215
Ile4	8.165	3.992	1.706	1.051, 1.303, 0.770
Leu5	8.206	4.207	1.495	0.770
Gln6	8.241	4.067	1.963, 1.846	2.197
Leu7	8.247	4.090	1.472	
Asn8	8.416	4.347	2.688, 2.547	
Leu9	8.039	4.160	1.472, 1.447	0.794, 0.724
Lys10	8.136	4.015	1.612	1.659, 1.261, 2.841, 7.339
Lys10b	7.990	4.020	1.565	1.659, 1.238
Glu11	8.133	4.135	1.823, 1.729	2.103
Tyr12	8.037	4.394	2.921, 2.781	
Tyr12b	8.107	4.418	2.898, 2.781	
Asn13	8.223	4.511	2.617, 2.524	
Asn13b	8.288	4.488	2.594, 2.500	
Leu14	8.007	4.182	1.470	
Val15	7.925	3.927	1.916	0.817, 0.794
Val15b	8.107	3.927	1.893	0.817, 0.794

(Figure 5A, i)] to 8.165 ppm [TP-bound Gαq-Ct peptide (Figure 5A, ii)] strongly suggested that the N-terminal segment of the Gαq-Ct peptide could bind to the purified TP with a low affinity. On the other hand, residues with slow exchange as characterized by the existence of two sets of peaks, representing the free and TP-bound forms of the Gαq-Ct peptide, were identified in the C-terminal segment of the Gαq-Ct peptide. The peaks for residues K10 and V15 in a similar region of the TOCSY spectrum are shown in panels B and C of Figure 5, respectively. In the absence of the TP, the amide protons of K10 and V15 have chemical shifts at 8.067 ppm (Figure 5B, i) and 7.872 ppm (Figure 5C, i), respectively, in the TOCSY spectrum. Upon addition of the purified TP to the peptide, each single set of chemical shifts for K10 and V15 was separated into two sets of chemical shifts (Figure 5B, ii, and Figure 5C, ii, respectively), which demonstrated a typical slow exchange behavior. The slow exchanges were strong evidence that the C-terminal segment of the Gαq-Ct peptide could bind to the purified TP with an affinity much higher than that of its N-terminal segment, as indicated by a fast exchange behavior as described above. This information has provided evidence showing that the Gαq-Ct peptide binds to the TP before agonist activation in the nonionic detergent-mimicked lipid environment. In addition, the observation of fast exchange in the N-terminal residue (Figure 5A) and slow exchange in the C-terminal residues (Figure 5B,C) of the Gαq-Ct peptide has suggested that the binding of the Gαq-Ct peptide to the ligand-free TP is likely through its C-terminal segment rather than the N-terminal segment.

NMR Study of the Interaction between the Gαq-Ct Peptide and the Agonist (U46619)-Activated TP in a Lipid Environment. 2D proton NMR experiments were performed for the Gαq-Ct peptide in the presence of the purified TP, activated by 10 μM agonist U46619. The complete resonance assignments of HN, Hα, Hβ, and others for the Gαq-Ct peptide in the presence of U46619-activated TP are listed in Table 3. Most of the peaks in the TOCSY spectrum of the peptide were similar to those of the ligand-free TP-bound Gαq-Ct peptide, except for the peaks of N8, which became very weak, perhaps due to intermediate exchange-induced line broadening. However, for those residues undergoing fast exchange, the difference in chemical shift compared with that of a free peptide became smaller.

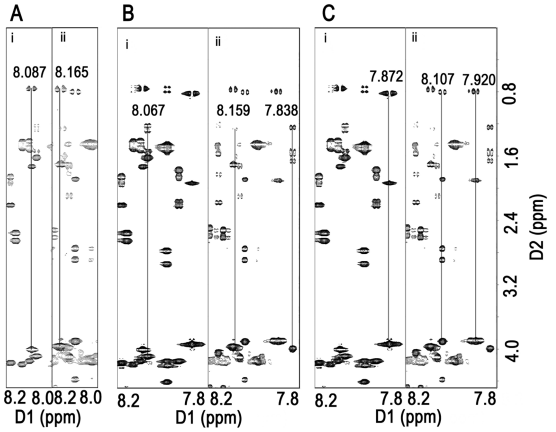

FIGURE 5: TOCSY spectra for the free and bound Gαq-Ct peptide upon interaction with agonist-free TP. Comparison of TOCSY peaks for residues I4 (A), K10 (B), and V15 (C) of the free Gαq-Ct peptide (part i) and the Gαq-Ct peptide in the presence of ligand-free TP (part ii). Only a single set of peaks for residue I4 was observed in panel A, whereas two sets of cross-peaks could be observed for K10 (B) and V15 (C) in the spectrum of the Gαq-Ct peptide in the presence of ligand-free TP. The peaks at the D1 position (7.838 ppm) in panel B and the peaks at the D1 position (8.107 ppm) in panel C are from the bound forms of K10 and V15, respectively.

Table 3: Proton Chemical Shifts for the Gαq-CT Peptide in the Presence of U46619-Activated TP

residue	HN	Hα	Hβ	others
Lys1		3.875	1.776	1.565, 1.309, 2.870, 7.417
Asp2	8.785	4.629	2.712, 2.594	
Thr3	8.259	4.161	4.021	1.052
Ile4	8.095	4.021	1.706	1.332, 1.029, 0.707, 0.748
Leu5	8.194	4.208	1.449	1.426, 0.771, 0.725
Gln6	8.223	4.202	1.940, 1.847	2.197
Leu7	8.235	4.231	1.490, 1.426	0.771, 0.725
Asn8			unassigned	
Leu9	8.031	4.185	1.472, 1.447	0.794, 0.724
Lys10	8.136	4.091	1.613	
Lys10b	7.990	4.068	1.706	1.613, 1.261, 2.841, 7.399
Glu11	8.042	4.115	1.823, 1.729	2.174
Tyr12	8.048	4.418	2.922, 2.759	6.967
Tyr12b	8.112	4.418	2.922, 2.759	
Asn13	8.218	4.512	2.641, 2.548	
Asn13b	8.282	4.511	2.595, 2.501	
Leu14	8.001	4.182	1.519, 1.449	
Val15	7.925	3.927	1.916	0.817, 0.794
Val15b	8.095	3.927		

Figure 6A shows the TOCSY peaks for residue I4 in the presence of the U46619-activated TP receptor. The difference between part ii of Figure 5A (peptide with the ligand-free receptor) and part i of Figure 5A (free peptide) was 0.078 ppm, while for parts i and ii of Figure 6A, the difference was 0.014 ppm. On the other hand, the peak intensity for the bound peptide decreased in those residues undergoing slow exchange, shown in panels B and C of Figure 6. It was clearly observed that in part ii of Figure 6B, the relative peak intensity of K10 in the bound peptide (7.990 ppm) was weaker than that in part ii of Figure 5B (7.838 ppm). Also, clear differences can be observed between part ii of Figure 6C and part ii of Figure 5C. In addition, as indicated in part ii of Figure 6C, which showed the signals of V15, only the HN-Hα cross-peaks could be observed at the bottom of the line for the bound peptide, while in part ii of Figure 5C, similar intensities were observed for the free and bound peptides. All of the changes

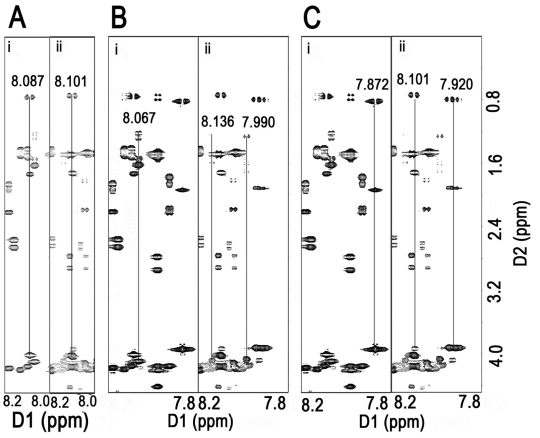

FIGURE 6: TOCSY spectra for the free and bound Gαq-Ct peptide upon interaction with agonist-activated TP. Comparison of TOCSY peaks for residues I4 (A), K10 (B), and V15 (C) of the free Gαq-Ct peptide (part i) and the Gαq-Ct peptide in the presence of the U46619-activated receptor (part ii). Fewer shifts could be observed for residue I4 compared to the number in Figure 5. The peaks from the bound peptide (7.990 ppm for K10 and 8.101 ppm for V15) became weaker in comparison to that in Figure 5.

described above indicated an overall weakened binding for the agonist-bound TP when compared with that of the agonist-free TP, which is consistent with the fluorescence spectroscopy study described above (Figure 2).

It should also be noted that an alternative way to explain the fast and slow exchange in the NMR experiments for the Gαq-Ct peptide binding to TP is to have two binding modes between the Gαq-Ct peptide and TP in solution, one binding strongly and the other weakly. It is reasonable to predict that most forms of Gq-Ct bound to the TP are in the strong mode because this should have better competitive binding compared to that of the weak binding mode in general.

Solution Structures of the Gαq-Ct Peptide Bound to TP in the Absence and Presence of the Receptor Agonist. The solution structures of the Gαq-Ct peptide, bound to the TP in the absence and presence of the agonist, U46619, were further determined by the NOE constraints calculated from the NOESY spectra using 2D ^{1}H NMR spectroscopy. The numbers of constraints per residues for these two structure calculations are summarized in panels B and C of Figure 7. Fifty initial structures were calculated with DG II, and 10 structures with the smallest rmsd were chosen. The rmsd values for the structures of the Gαq-Ct peptide with unstimulated TP and U46619-stimulated TP were 1.4 and 1.6 Å, respectively. Average energy values for the structures of the peptide with unstimulated TP and U46619-stimulated TP were 135 and 197 kcal/mol, respectively. Through the complete assignments of the TOCSY and NOESY spectra for the Gαq-Ct peptide, with and without U46619, in the presence of medium-range NOEs in the C-terminal residues of the ligand-free TP-bound Gαq-Ct peptide, the existence of a helical structure similar to that of the free form of the peptide has been indicated. The absence of medium-range NOEs at the N-terminus of the peptide indicates a significant probability that the Gαq-Ct peptide is a random coil structure (data not shown). The ligand-free, TP-bound 3D structure of the Gαq-Ct peptide, calculated with DG II, is shown in Figure 8A. The N-terminal segment of this bound state Gαq-Ct peptide became a random coil structure as predicted, whereas the C-terminus remained a helical structure, with a half-turn located from L7 to K10 (Figure 8A). In the NOESY spectrum of the U46619-activated TP, a few medium-range NOEs could be identified. The calculated 3D structure of the Gαq-Ct peptide, bound to the U46619-activated TP, is shown in Figure 8B. The N-terminus of the peptide once again becomes a short helical structure followed by a random coil structure in the middle and a C-terminal short helix. This is also different from the structure of the Gαt C-terminal peptide's binding to light-activated rhodopsin, which has a very unusual "turn back" structure, also defined as "C-Cap" (*12*).

Establishing a Cell Line That Stably Expresses Human TP. HEK293 cells were transfected with cloned human TP cDNA in the pcDNA3.1 vector using Lipofectamine2000 as described previously (*39*). A cell line stably expressing the human TP (TP stable cell line) was generated by G418 screening after 2 months (*41*). The recombinant human TP expressed in the cells was confirmed by Western blot analysis using the purified TP as a standard (Figure 9A). The TP expression level was 0.01 pmol/20 μg of protein for TP in HEK293 as a stable cell line.

Determination of the Ligand-Free Constitutive TP Signaling through Gq Coupling. The cytoplasmic calcium concentrations for the TP stable cell line and HEK293 cells have been quantitatively measured to be approximately 125 and 40 nM, respectively (*42*, *43*) (Figure 9B). This 3-fold difference could be used to monitor the calcium signaling mediated by the over-expressed recombinant receptor in the cells (*44*).

The Gq-mediated calcium signaling activity as calcium concentration of the human TP expressed in the stable cell line was confirmed by a fluorescence calcium signaling assay using U46619 as a specific TP agonist. The ligand-free constitutive TP signaling (through binding to Gq) was identified by the following evidence. (1) The basal level of the fluorescence intensity as calcium concentration that resulted from the influx of calcium bound to Fluo8 in the TP stable cell line was 2-fold higher compared to that of the nontransfected control cells (Figure 9B). (2) The higher level of basal calcium signaling in the TP stable cell line was also supported by longer photobleaching (Figure 9C). (3) The stronger influx of calcium signaling in the TP stable cell line was almost completely blocked by the TP antagonist, SQ29,548 (Figure 9B,C). The vector-transfected controls were similar to HEK293 controls. This clearly indicated that the increased calcium influx in the TP stable cell line is mediated by the over-expressed human TP (Figure 9B,C).

DISCUSSION

Previously, it was reported that the peptide corresponding to the C-terminus of Gαt is highly disordered in the absence of rhodopsin (*12*), and its NOESY spectra had virtually no cross-peaks. However, considering the differences between the amino acid sequences of the C-terminal domains of Gαt (CGLF) and Gαq (YNLV), it was no surprise to see that there were also differences in the helical structure configuration for Gαq-Ct and Gαt. The comparison of the various Gα-Ct termini shows that there are very few residues conserved among Gαs, Gαi, and Gαq (Figure 10).

From a chimerical protein study that was performed with the Gαq protein, Conklin et al. (*20*) determined that by changing the last three residues of Gαq into the corresponding residues of Gαt and Gαi, this was sufficient to make the Gαq couple to those receptors that initially coupled to the Gt and Gi protein. This means that the 3D structure of the Gαq C-terminal domain should be quite different from that of Gαt and Gαi, which was confirmed by our studies. The helical structure of the Gαq

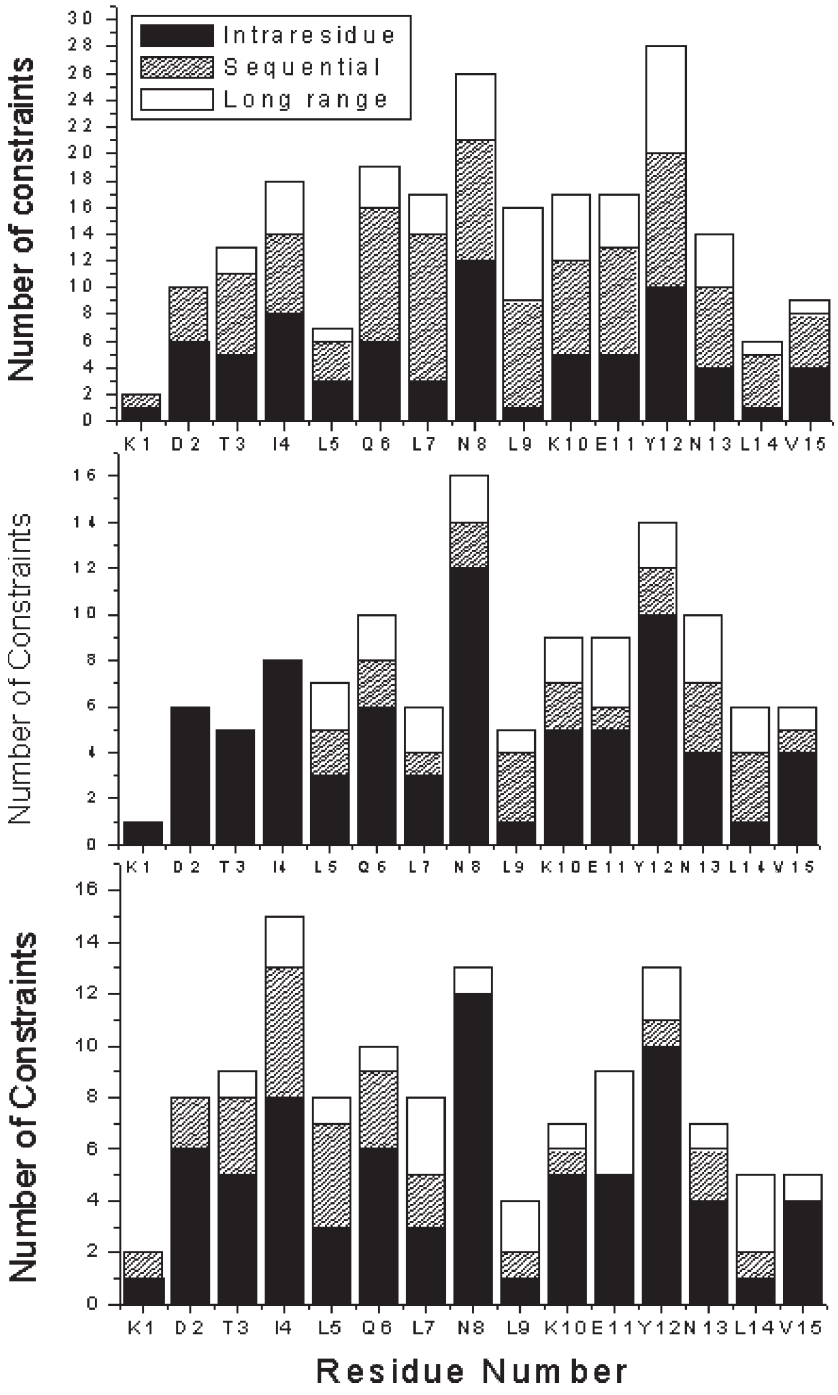

FIGURE 7: NOE constraints calculated from NOESY spectra using 2D ^{1}H NMR spectroscopy. Number of constraints per residue for the Gαq-Ct peptide in the absence (A) and presence (B) of the TP and in the presence of U46619-activated TP (C). Intraresidue, sequential, and long-range NOEs are shown with black, hatched, and white bars, respectively.

C-terminal domain most likely keeps it from fitting into those receptors that predominantly couple to Gαt and Gαi. This difference in the C-terminal structures provides a reasonable explanation for the different G-protein coupling preferences in different GPCRs. It is clear that the mechanisms for the Gαq C-terminal domain's binding to the agonist-free TP are different from that of Gαt C-terminal domain's binding to rhodopsin in the same family of GPCRs, which becomes an interesting issue that needs to be further investigated and characterized. The NMR structure of the Gα peptide may not be identical to that of the structure in the native protein. Thus, the NMR peptide structure is an initial structural characterization, which needs to be confirmed by protein crystallization.

Historically, the original ternary complex model described the presence of a ligand−receptor−G-protein complex, and it was assumed that GPCRs (without agonist stimulation) did not bind or activate the G-protein (*45*). However, the discovery of constitutive activity and inverse agonism phenomena (*11*, *46*) with many GPCRs led to the manifestation of an extended ternary complex (ETC) model, in which the ligand-free receptors are assumed to have both an active conformation state and inactive conformation state, of which the active state can couple to the G-protein (*11*, *47*). Further experimental observation revealed the presence of nonsignaling antagonist−GPCR−G-protein complexes. This revelation led to the extension of the ETC model to a cubic ternary complex (CTC) model that allows the inactive

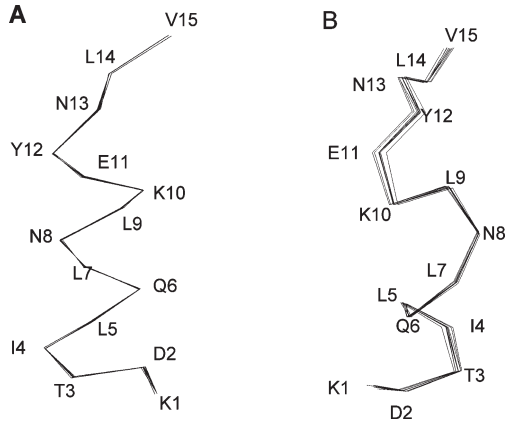

FIGURE 8: Ligand-free TP-bound 3D structure of the Gαq-Ct peptide. Eight superimposed 3D structures were generated from DG II and molecular dynamics calculations for the Gαq-Ct peptide bound to the ligand-free TP receptor (A) and Gαq-Ct peptide bound to U46619-activated TP (B).

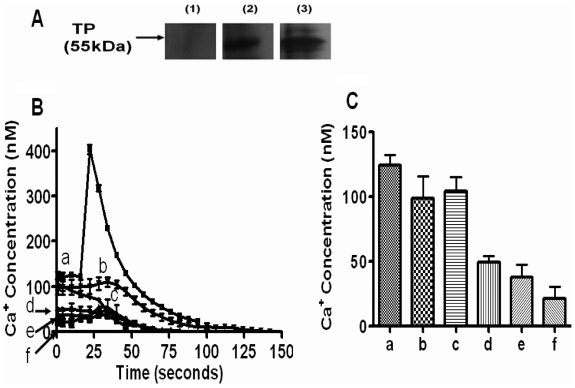

FIGURE 9: Recombinant human TP expression and its basal calcium signaling activity with the TP agonist U46619. (A) Western blot analysis. The membrane proteins were separated by 10% SDS−PAGE, and then Western blot analysis was performed using a human TP polyclonal antibody as described in Experimental Procedures. The correct molecular mass of the recombinant human TP (55 kDa) was identified by the bands in (1) HEK293 cells only as controls, (2) the TP stable cell line in HEK293 cells, and (3) TP in Sf9 cells. The specific fluorescence intensity as calcium concentration was determined as described previously (*51*) using HEK293 cells stably overexpressing the TP protein (TP stable cell line). (B) Time course of the signaling and fluorescence changes ($n = 3$), where the time taken for the basal calcium signal to photobleach is represented on the *x*-axis. (a) The agonist U46619 (80 nM) was added, and all values were recorded ($n = 3$). TP mediated basal calcium concentration. The HEK293 cells stably expressing human TP in the absence (b) and presence (c) of TP antagonist SQ29,548 (~1 μM). Untransfected HEK293 cells (d), HEK293 cells stably expressing microsomal prostaglandin E2 synthase-1 (mPGES-1) (e), and an empty vector (f) were loaded with Fluo8 for 20 min. After the cells had been washed, the basal level calcium signaling was initiated by perturbation of cells using gentle shaking (10 times), and then the cells were observed by fluorescence microscopy, which is designed for the calcium signaling assay. (C) Baselines for the specific fluorescence intensity as calcium concentration of each cell type (as indicated) were determined prior to the initiation of photobleaching ($n = 3$).

receptor to couple with the G-protein (*11*, *48*). The ETC (not shown) and CTC models in pharmacological receptor theory have also hypothesized the presence of such binding as the R_aG (ligand-free receptor active state binding G-protein) or R_iG (ligand-free receptor inactive state binding but not activating G-protein) state (*46*, *47*). Our study, however, provided direct spectroscopic evidence that the C-terminal domain of Gαq binds

RDIIQRMHLR-QYELL	G αs
TDVIIKNNLK-DCGLF	Gαi
KDTILQLNLK-EYNLV	G α q, or 11
KDTILQENLK-DIMLQ	G α12
KDTILHDNLK-QLMLQ	G α13
KDTILQLNLR-EFNLV	G α14
RDSVLARYLD-EINLL	G α15

FIGURE 10: Sequence alignment of the C-terminal domains of the various Gα proteins. The highlighted residues are the conserved residues.

to the TP without the agonist. Our previous studies reported that a mini-gene technique was used to coexpress the 11-residue peptide of the Gαq, which was able to block the receptor signaling via Gq coupling (*40*). This suggests the existence of a preoccupied G-protein binding site on the intracellular domains of the ligand-free TP. The data obtained from the study also suggested that the last six residues of the Gαq-Ct peptide are more important for the molecular recognition between TP and the Gαq protein because they bind to TP with an affinity higher than that for other residues. Our next effort will be directed at studying the interaction of TP in the presence of an antagonist.

The high-resolution structures available for rhodopsin and the β-2 adrenergic receptor provide valuable support for this study. In comparison with rhodopsin, the β-2 receptor has been shown to have a more open arrangement of the transmembrane domain (*49*, *50*). It is believed that the more closed structure of rhodopsin forces the charged residues (on the intracellular loops) to form an "ionic lock" which effectively shuts off any possible basal activity. In contrast, the more open structure of the β-2 receptor breaks this ionic lock so that it has basal activity. Because the sequence similarity of TP is higher with the β-2 receptor than with rhodopsin, it is reasonable to believe that TP also possesses basal activity. This is of prime importance because TP is ubiquitously present in the body and could maintain homeostasis and produce various pathological states with such basal activity. A ligand could enhance, weaken, or induce the reversal (inverse agonism) of this basal activity. Ultimately, drugs could be developed to form ligand-specific receptor active states and thus "select" certain signaling pathways. More extensive research will be required to achieve this long-term goal.

Recently, the crystal structure of the complex of Gαq and p63RhoGEF was determined at a low resolution (3.5 Å). Part of the C-terminus of Gαq showed a helical structure, which is similar to that of the determined C-terminal Gαq. The NMR study could also provide the dynamic structural changes in the C-terminal Gαq in the process of interacting with a GPCR, which is difficult in the determination of the crystal structure.

It should also be noted that the chemical shift perturbations used to compare the binding of the Gq-Ct peptide to the TP and agonist-activated TP assume a similar binding mode and pocket, which are generally observed for the interaction between the G-protein and GPCRs.

The TP stable cell line showed a higher calcium influx of signaling mediated by Gq coupling (Figure 9), which strongly supported our NMR results. Such findings indicate a promising new outlook for studying GPCR−G-protein interactions in greater detail using the integrated approaches of NMR spectroscopy, purified prostanoid receptors, and recombinant cell lines.

The native TP receptor in cells such as platelets is more complicated because the cells contain different receptors. The constitutive TP activity exhibited by the HEK cells overexpressing recombinant TP is likely to be different from that of the endogenous TP expressed in the regular cells because the levels of the expressed

TP in cells could be different. Testing the constitutive activity of the endogenous TP in the regular cells would be part of the future study for the project. Though the agonist binding significantly weakens the interaction between the receptor and the C-terminus of Gαq, it will be interesting to further explore what the consequences for the signaling pathway at the molecular level would be. We suggest that the differences in signaling mechanisms might be beneficial for differentiating among agonists, inverse agonists, and antagonists.

Thus, the biological speculation about the results obtained from structure and function characterization for the interaction between TP and Gq needs to be investigated using native cells.

ACKNOWLEDGMENT

Acknowledgement is made to Dr. Xiaolian Gao and Dr. Youlin Xia in the Department of Biology and Biochemistry and the Keck NMR Center, University of Houston, for access to the NMR facilities.

REFERENCES

1. Funk, C. D. (2001) Prostaglandins and leukotrienes: Advances in eicosanoid biology. *Science 294*, 1871–1875.
2. Majerus, P. W. (1983) Arachidonate metabolism in vascular disorders. *J. Clin. Invest. 72*, 1521–1525.
3. Miller, D. K., Sadowski, S., Soderman, D. D., and Kuehl, F. A., Jr. (1985) Endothelial cell prostacyclin production induced by activated neutrophils. *J. Biol. Chem. 260*, 1006–1014.
4. Negishi, M., Sugimoto, Y., and Ichikawa, A. (1995) Molecular mechanisms of diverse actions of prostanoid receptors. *Biochim. Biophys. Acta 1259*, 109–120.
5. Coleman, R. A., Kennedy, I., Humphrey, P. P. A., Bunce, K., and Kumley, P. (1990) Prostanoid and their receptor. In Comprehensive Medicinal Chemistry (Hansch, C., Sammes, P. G., Taylor, J. B., and Emmett, J. C., Eds.) Vol. *3*, pp 643−714, Pergamon Press, Oxford, U.K.
6. Ushikubi, F., Nakajima, M., Hirata, M., Okuma, M., Fujiwara, M., and Narumiya, S. (1989) Purification of the thromboxane A2/prostaglandin H2 receptor from human blood platelets. *J. Biol. Chem. 264*, 16496–16501.
7. Hirata, M., Hayashi, Y., Ushikubi, F., Yokata, Y., Kageyama, R., Nakanishi, S., and Narumiya, S. (1991) Cloning and expression of cDNA for a human thromboxane A2 receptor. *Nature 349*, 617–620.
8. Raychowdhury, M. K., Yukawa, M., Collins, L. J., McGrail, S. H., Kent, K. C., and Ware, J. A. (1994) Alternative splicing produces a divergent cytoplasmic tail in the human endothelial thromboxane A2 receptor. *J. Biol. Chem. 269*, 19256–19261.
9. Huang, J. S., Ramamurthy, S. K., Lin, X., and Le Breton, G. C. (2004) Cell signaling through thromboxane A2 receptors. *Cell. Signalling 16*, 521–533.
10. Walsh, M., Foley, J. F., and Kinsella, B. T. (2000) Investigation of the role of the carboxyl-terminal tails of the α and β isoforms of the human thromboxane A_2 receptor (TP) in mediating receptor: Effector coupling. *Biochim. Biophys. Acta 1496*, 164–182.
11. Kenakin, T. (2004) Principles: Receptor theory in pharmacology. *Trends Pharmacol. Sci. 25*, 186–192.
12. Kisselev, O. G., Kao, J., Ponder, J. W., Fann, Y. C., Gautam, N., and Marshall, G. R. (1998) Light-activated rhodopsin induces structural binding motif in G protein α subunit. *Proc. Natl. Acad. Sci. U.S.A. 95*, 4270–4275.
13. Tesmer, V. M., Kawano, T., Shankaranarayanan, A., Kozasa, T., and Tesmer, J. J. (2005) Snapshot of activated G proteins at the membrane: The Gαq-GRK2-G$\beta\gamma$ complex. *Science 310*, 1686–1690.
14. Lutz, S., Shankaranarayanan, A., Coco, C., Ridilla, M., Nance, M. R., Vettel, C., Baltus, D., Evelyn, C. R., Neubig, R. R., Wieland, T., and Tesmer, J. J. (2007) Structure of Gαq-p63RhoGEF-RhoA complex reveals a pathway for the activation of RhoA by GPCRs. *Science 318*, 1923–1927.
15. Dratz, E. A., Furstenau, J. E., Lambert, C. G., Thireault, D. L., Rarick, H., Schepers, T., Pakhlevaniants, S., and Hamm, H. E. (1993) NMR structure of a receptor-bound G-protein peptide. *Nature 363*, 276–281.
16. Ridge, K. D., Marino, J. P., Ngo, T., Ramon, E., Brabazon, D. M., and Abdulaev, N. G. (2006) NMR analysis of rhodopsin-transducin interactions. *Vision Res. 46*, 4482–4492.
17. Abdulaev, N. G., Ngo, T., Zhang, C., Dinh, A., Brabazon, D. M., Ridge, K. D., and Marino, J. P. (2005) Heterotrimeric G-protein α-subunit adopts a "preactivated" conformation when associated with $\beta\gamma$-subunits. *J. Biol. Chem. 280*, 38071–38080.
18. Ridge, K. D., Abdulaev, N. G., Zhang, C., Ngo, T., Brabazon, D. M., and Marino, J. P. (2006) Conformational changes associated with receptor-stimulated guanine nucleotide exchange in a heterotrimeric G-protein α-subunit: NMR analysis of GTPγS-bound states. *J. Biol. Chem. 281*, 7635–7648.
19. Piscitelli, C. L., Angel, T. E., Bailey, B. W., Hargrave, P., Dratz, E. A., and Lawrence, C. M. (2006) Equilibrium between metarhodopsin-I and metarhodopsin-II is dependent on the conformation of the third cytoplasmic loop. *J. Biol. Chem. 281*, 6813–6825.
20. Conklin, B. R., Farfel, Z., Lustig, K. D., Julius, D., and Bourne, H. R. (1993) Substitution of three amino acids switches receptor specificity of Gqα to that of Giα. *Nature 363*, 274–276.
21. Ruan, K. H., Cervantes, V., and Wu, J. (2008) A simple, quick, and high-yield preparation of the human thromboxane A2 receptor in full size for structural studies. *Biochemistry 47*, 6819–6826.
22. Hamm, H. E., Deretic, D., Arendt, A., Hargrave, P. A., Koenig, B., and Hofmann, K. P. (1998) Site of G protein binding to rhodopsin mapped with synthetic peptides from the α subunit. *Science 241*, 832–835.
23. Albrizio, S., Caliendo, G., D'errico, G., Novellino, E., Rovero, P., and D'ursi, A. M. (2005) Gα(s) protein C-terminal α-helix at the interface: Does the plasma membrane play a critical role in the Gα(s) protein functionality? *J. Pept. Sci. 11*, 617–626.
24. Sunahara, R. K., Tesmer, J. J., Gilman, A. G., and Sprang, S. R. (1997) Crystal structure of the adenylyl cyclase activator Gsα. *Science 278*, 1943–1947.
25. Dursi, A. M., Albrizio, S., Greco, G., Mazzeo, S., Mazzoni, M. R., Novellino, E., and Rovero, P. (2002) Conformational analysis of the $G\alpha_s$ protein C-terminal region. *J. Pept. Sci. 8*, 476–488.
26. Albrizio, S., D'Ursi, A., Fattorusso, C., Galoppini, C., Greco, G., Mazzoni, M. R., Novellino, E., and Rovero, P. (2000) Conformational studies on a synthetic C-terminal fragment of the α subunit of G_S proteins. *Biopolymers 54*, 186–194.
27. Mazzoni, M. R., Taddei, S., Giusti, L., Rovero, P., Galoppini, C., D'Ursi, A., Albrizio, S., Triolo, A., Novellino, E., Greco, G., Lucacchini, A., and Hamm, H. E. (2000) A $G\alpha_s$ carboxylterminal peptide prevents G_s activation by the A_{2A} adenosine receptor. *Mol. Pharmacol. 58*, 226–236.
28. Masters, S. B., Sullivan, K. A., Miller, R. T., Beiderman, B., Lopez, N. G., Ramachandran, J., and Bourne, H. R. (1988) Carboxyl terminal domain of Gsα specifies coupling of receptors to stimulation of adenylyl cyclase. *Science 241*, 448–451.
29. Rasenick, M. M., Watanabe, M., Lazarevic, M. B., Hatta, S., and Hamm, H. E. (1994) Synthetic peptides as probes for G protein function. Carboxyl-terminal Gαs peptides mimic Gs and evoke high affinity agonist binding to β-adrenergic receptors. *J. Biol. Chem. 269*, 21519–21525.
30. Feldman, D. S., Zamah, A. M., Pierce, K. L., Miller, W. E., Kelly, F., Rapacciuolo, A., Rockman, H. A., Koch, W. J., and Luttrell, L. M. (2002) Selective inhibition of heterotrimeric Gs signaling. Targeting the receptor-G protein interface using a peptide minigene encoding the $G\alpha_s$ carboxyl terminus. *J. Biol. Chem. 277*, 28631–28640.
31. Zhang, L., Huang, G., Wu, J., and Ruan, K. H. (2005) A profile of the residues in the first intracellular loop critical for Gs-mediated signaling of human prostacyclin receptor characterized by an integrative approach of NMR-experiment and mutagenesis. *Biochemistry 44*, 11389–11401.
32. Wüthrich, K. (1986) NMR of Proteins and Nucleic Acids, Wiley, New York.
33. Lippens, R. M., Cerf, C., and Hallenga, K. (1992) Theory and experimental results of transfer-NOE experiments. The influence of the off rate versus cross-relaxation rates. *J. Magn. Reson. 99*, 268–281.
34. Landy, S. B., and Rao, B. D. N. (1989) Dynamical NOE in multiple-spin systems undergoing chemical exchange. *J. Magn. Reson. 81*, 371–377.
35. Ruan, K. H., Wu, J., and Wang, L. H. (2005) Solution structure of a common substrate mimetic of cyclooxygenase-downstream synthases bound to an engineered thromboxane A2 synthase using a high-resolution NMR technique. *Arch. Biochem. Biophys. 444*, 165–173.
36. Ruan, K. H., Wu, J., and Cervantes, V. (2008) Characterization of the substrate mimic bound to engineered prostacyclin synthase in solution using high-resolution NMR spectroscopy and mutagenesis: Implication of the molecular mechanism in biosynthesis of prostacyclin. *Biochemistry 47*, 680–688.
37. Callihan, D., West, J., Kumar, S., Schweitzer, B. I., and Logan, T. M. (1996) Simple, distortion-free homonuclear spectra of peptides and

nucleic acids in water using excitation sculpting. *J. Magn. Reson., Ser. B 112*, 82–85.
38. Marion, D., Ikura, M., Tschudin, R., and Bax, A. (1989) Rapid recording of 2D NMR spectra withoutphase cycling. Application to the study of hydrogen exchange in proteins. *J. Magn. Reson. 85*, 393–399.
39. Ruan, K. H., Deng, H., and So, S. P. (2006) Engineering of a protein with cyclooxygenase and prostacyclin synthase activities that converts arachidonic acid to prostacyclin. *Biochemistry 45*, 14003–14011.
40. Gilchrist, A., Vanhauwe, J. F., Li, A., Thomas, T. O., Voyno-Yasenetskaya, T., and Hamm, H. E. (2001) Gα minigenes expressing C-terminal peptides serve as specific inhibitors of thrombin-mediated endothelial activation. *J. Biol. Chem. 276*, 25672–25679.
41. Ruan, K. H., So, S. P., Cervantes, V., Wu, H., Wijaya, C., and Jentzen, R. R. (2008) An active triple-catalytic hybrid enzyme engineered by linking cyclo-oxygenase isoform-1 to prostacyclin synthase that can constantly biosynthesize prostacyclin, the vascular protector. *FEBS J. 275*, 5820–5829.
42. Pinto, A., Gillard, S., Moss, F., Whyte, K., Brust, P., Williams, M., Stauderman, K., Harpold, M., Lang, B., Newsom-Davis, J., Bleakman, D., Lodge, D., and Boot, J. (1998) Human autoantibodies specific for the a1A calcium channel subunit reduce both P-type and Q-type calcium currents in cerebellar neurons. *Proc. Natl. Acad. Sci. U.S.A. 95*, 8328–8333.
43. Kao, J. P., Harootunian, A. T., and Tsien, R. Y. (1989) Photochemically Generated Cytosolic Calcium Pulses and Their Detection by Fluo-3. *J. Biol. Chem. 264*, 8179–8184.
44. Huang, J., Hamasaki, T., and Ozoe, Y. (2009) Pharmacological characterization of a *Bombyx mori* α-adrenergic-like octopamine receptor stably expressed in a mammalian cell line. *Arch. Insect Biochem. Physiol. 73*, 74–86.
45. De Lean, A., Stadel, J. M., and Lefkowitz, R. J. (1980) A ternary complex model explains the agonist-specific binding properties of the adenylate cyclase-coupled β-adrenergic receptor. *J. Biol. Chem. 255*, 7108–7117.
46. Costa, T., and Herz, A. (1989) Antagonists with negative intrinsic activity at δ opioid receptors coupled to GTP-binding proteins. *Proc. Natl. Acad. Sci. U.S.A. 86*, 7321–7325.
47. Samama, P., Cotecchia, S., Costa, T., and Lefkowitz, R. J. (1993) A mutation-induced activated state of the β2-adrenergic receptor. Extending the ternary complex model. *J. Biol. Chem. 26*, 4625–4636.
48. Brown, G. P., and Pasternak, G. W. (1998) ^{3}H-Naloxone benzoylhydrazone binding in MOR-1-transfected Chinese hamster ovary cells: Evidence for G-protein-dependent antagonist binding. *J. Pharmacol. Exp. Ther. 286*, 376–381.
49. Cherezov, V., Rosenbaum, D. M., Hanson, M. A., Rasmussen, S. G., Thian, F. S., Kobilka, T. S., Choi, H. J., Kuhn, P., Weis, W. I., Kobilka, B. K., and Stevens, R. C. (2007) High-resolution crystal structure of an engineered human β2-adrenergic G protein-coupled receptor. *Science 318*, 1258–1265.
50. Rasmussen, S. G., Choi, H. J., Rosenbaum, D. M., Kobilka, T. S., Thian, F. S., Edwards, P. C., Burghammer, M., Ratnala, V. R., Sanishvili, R., Fischetti, R. F., Schertler, G. F., Weis, W. I., and Kobilka, B. K. (2007) Crystal structure of the human β2 adrenergic G-protein-coupled receptor. *Nature 450*, 383–387.
51. Gee, K. R., Brown, K. A., Chen, W. N., Bishop-Stewart, J., Gray, D., and Johnson, I. (2000) Chemical and physiological characterization of fluo-4 Ca^{2+}-indicator dyes. *Cell Calcium 27*, 97–106.